Physics Letters B 761 (2016) 456–461

Contents lists available at ScienceDirect

Physics Letters B

www.elsevier.com/locate/physletb

The electromagnetic form factors of the Λ in the timelike region

J. Haidenbauer [a], U.-G. Meißner [b,a]

[a] Institute for Advanced Simulation, Institut für Kernphysik and Jülich Center for Hadron Physics, Forschungszentrum Jülich, D-52425 Jülich, Germany
[b] Helmholtz Institut für Strahlen- und Kernphysik and Bethe Center for Theoretical Physics, Universität Bonn, D-53115 Bonn, Germany

ARTICLE INFO

Article history:
Received 10 August 2016
Received in revised form 31 August 2016
Accepted 31 August 2016
Available online 6 September 2016
Editor: J.-P. Blaizot

Keywords:
Electromagnetic form factors
Hadron production in e^+e^- interactions
$\bar{\Lambda}\Lambda$ interaction

ABSTRACT

The reaction $e^+e^- \to \bar{\Lambda}\Lambda$ is investigated for energies close to the threshold. Specific emphasis is put on the role played by the interaction in the final $\bar{\Lambda}\Lambda$ system which is taken into account rigorously. For that interaction a variety of $\bar{\Lambda}\Lambda$ potential models is employed that have been constructed for the analysis of the reaction $\bar{p}p \to \bar{\Lambda}\Lambda$ in the past. The enhancement of the effective form factor for energies close to the $\bar{\Lambda}\Lambda$ threshold, seen in pertinent experiments, is reproduced. Predictions for the Λ electromagnetic form factors G_M and G_E in the timelike region and for spin-dependent observables such as spin-correlation parameters are presented.

1. Introduction

The electromagnetic form factors (EMFF) of the nucleon in the timelike region have been studied intensively over the last few years, see the recent review [1]. Information on these quantities is accessible in the $\bar{p}p$ annihilation process $\bar{p}p \to e^+e^-$ [2], and likewise in the reactions $e^+e^- \to \bar{p}p$ and $e^+e^- \to \bar{n}n$ from where most of the recent data emerged [3,4] and where experimental efforts continue [5–7]. New experiments for $\bar{p}p \to e^+e^-$ are in planning [8]. One particular feature that attracted wide attention was the observation of a strong enhancement of the proton EMFFs close to the $\bar{p}p$ threshold, i.e. at momentum transfers $q^2 \simeq (2M_p)^2$. This behavior was first detected in the PS170 experiment [2], in a measurement of $\bar{p}p \to e^+e^-$ at the CERN Low Energy Antiproton Ring (LEAR), and confirmed in recent years in experiments with high mass resolution by the BaBar collaboration for the time-reversed process $e^+e^- \to \bar{p}p$ [3,4]. The majority of theoretical studies [9–16] attributed this strong enhancement to effects of the $\bar{p}p$ interaction in the final state. This final state interaction (FSI) enhances the near-threshold $e^+e^- \to \bar{p}p$ cross section as compared to the phase space and, in turn, yields (effective) proton EMFFs that peak at the threshold and then fall off rapidly with increasing energy. Refined calculations of the $e^+e^- \to \bar{p}p$ cross section (and/or EMFFs) like the one performed by us [14] yield results that are in excellent agreement with the near-threshold data. The study in Ref. [14] relies on a formally exact treatment of the effects from the $\bar{p}p$ interaction in the final state, and utilizes $\bar{N}N$ potentials constructed in the framework of chiral effective field theory [17] and fitted to results of a partial wave analysis of $\bar{p}p \to \bar{p}p$ and $\bar{p}p \to \bar{n}n$ scattering data [18].

In the present paper we take a look at the electromagnetic form factors in the timelike region of another baryon, namely those of the Λ hyperon. In this case much less measurements have been published [19–22] (and with significantly lower mass resolution) and there are only few theoretical studies [11,13,23,24]. Anyway, the available data suggest that the Λ form factor exhibits a near-threshold behavior very much similar to that of the proton [20]. Therefore, it is interesting to see whether we can reproduce that property within the same framework we have set up and employed successfully to the proton form factor [14]. Another and equally important motivation for our study is ongoing pertinent experiments by the BESIII collaboration at the BEPCII e^+e^- collider in Beijing. In this experiment, the self-analyzing character of the weak decay $\Lambda \to p\pi^-$ will be exploited so that it is possible to determine also the polarization as well as spin-correlation parameters for the reaction $e^+e^- \to \bar{\Lambda}\Lambda$ [22,25]. Those observables allow one to determine not only the (effective) form factor but also the relative magnitude of the two electromagnetic form factors G_M and G_E and even the phase between them [1,24]. Within our approach we can make predictions for those observables.

Our calculation for $e^+e^- \to \bar{\Lambda}\Lambda$ is done in complete analogy to the one for $e^+e^- \to \bar{p}p$ [14]. However, unlike the situation for $\bar{N}N$, there is no well established $\bar{\Lambda}\Lambda$ interaction potential available

E-mail address: j.haidenbauer@fz-juelich.de (J. Haidenbauer).

http://dx.doi.org/10.1016/j.physletb.2016.08.067

that can be used for the treatment of FSI effects. As a matter of fact, there is no direct information about the $\bar{\Lambda}\Lambda$ force at all. The only constraints one has for that interaction come from studies of FSI effects performed for another reaction, namely $\bar{p}p \to \bar{\Lambda}\Lambda$. This particular $\bar{p}p$ annihilation channel has been thoroughly investigated in the PS185 experiment at LEAR. Data are available (down to energies very close to the reaction threshold) for total and differential cross-sections but, thanks to the aforementioned self-analyzing weak Λ decay, also for spin-dependent observables [26–29]. In the present investigation we will resort to $\bar{\Lambda}\Lambda$ models that have been developed for the analysis of those PS185 data by us in the past [30–33]. Clearly, that introduces unavoidably a model dependence into our $e^+e^- \to \bar{\Lambda}\Lambda$ results. But at the present stage we rather view that as an advantage than a drawback. Considering various $\bar{\Lambda}\Lambda$ models, as we do here, allows us to shed light on the following questions: (1) which of the $e^+e^- \to \bar{\Lambda}\Lambda$ observables and, accordingly, which properties of the Λ EMFFs are only weakly influenced by detailed aspects of the $\bar{\Lambda}\Lambda$ interaction and, thus, can be established as being practically model-independent; (2) which quantities show a more pronounced sensitivity to variations of the $\bar{\Lambda}\Lambda$ interaction and, therefore, could provide useful information for pinning down the $\bar{\Lambda}\Lambda$ force more reliably in the future.

The paper is organized as follows: In Sect. 2 we describe briefly the employed formalism and in Sect. 3 we summarize the properties of the $\bar{\Lambda}\Lambda$ potential models used in the calculations. Numerical results for the $e^+e^- \to \bar{\Lambda}\Lambda$ reaction are presented in Sect. 4. We show results for observables such as total and differential cross section but also for spin-dependent quantities like the polarization and the spin-correlation parameters. In addition, our predictions for the electromagnetic form factors G_M and G_E are presented. The paper closes with a summary.

2. Formalism

Our formalism for the reaction $e^+e^- \to \bar{\Lambda}\Lambda$ is identical to the one developed and described in detail in Ref. [14] for the $e^+e^- \to \bar{p}p$ case. Therefore, we will be very brief here and define only the main quantities. We adopt the standard conventions so that the differential cross section for the reaction $e^+e^- \to \bar{\Lambda}\Lambda$ is given by [1]

$$\frac{d\sigma}{d\Omega} = \frac{\alpha^2\beta}{4s}\left[|G_M(s)|^2\,(1+\cos^2\theta) + \frac{4M_\Lambda^2}{s}\,|G_E(s)|^2\sin^2\theta\right]. \quad (1)$$

Here, $\alpha = 1/137.036$ is the fine-structure constant and $\beta = k_\Lambda/k_e$ a phase-space factor, where k_Λ and k_e are the center-of-mass three-momenta in the $\bar{\Lambda}\Lambda$ and e^+e^- systems, respectively, related to the total energy via $\sqrt{s} = 2\sqrt{M_\Lambda^2 + k_\Lambda^2} = 2\sqrt{m_e^2 + k_e^2}$. Further, M_Λ (m_e) is the Λ (electron) mass. G_M and G_E are the magnetic and electric form factors, respectively. The cross section as written in Eq. (1) results from the one-photon exchange approximation and by setting the electron mass m_e to zero (in that case $\beta = 2k_\Lambda/\sqrt{s}$). We will restrict ourselves throughout this work to the one-photon exchange so that the total angular momentum is fixed to $J = 1$ and the e^+e^- and $\bar{\Lambda}\Lambda$ system can be only in the partial waves $^3S_1$ and $^3D_1$. We use the standard spectral notation $^{(2S+1)}L_J$, where S is the total spin and L the orbital angular momentum. The tensor coupling between these two states is taken into account in our calculation.

The integrated reaction cross section is readily found to be

$$\sigma_{e^+e^-\to\bar{\Lambda}\Lambda} = \frac{4\pi\alpha^2\beta}{3s}\left[|G_M(s)|^2 + \frac{2M_\Lambda^2}{s}\,|G_E(s)|^2\right]. \quad (2)$$

Another quantity used in various analyses is the Λ effective form factor $G_{\rm eff}$ which is defined by

$$|G_{\rm eff}(s)| = \sqrt{\frac{\sigma_{e^+e^-\to\bar{\Lambda}\Lambda}(s)}{\frac{4\pi\alpha^2\beta}{3s}\left[1+\frac{2M_\Lambda^2}{s}\right]}}. \quad (3)$$

The spin-dependent observables such as the polarization P and the spin-correlation parameters C_{ij} are calculated within the formalism used in our study of $\bar{p}p \to \bar{\Lambda}\Lambda$. Explicit expressions can be found in the Appendix of Ref. [32] based on the general parameterization of the spin-scattering matrix for spin-1/2 particles [34]. Expressions for these spin-dependent observables in terms of the form factors G_M and G_E can be found in Ref. [24], see also [35,36].

3. The $\bar{\Lambda}\Lambda$ interaction

As already said in the Introduction, the $\bar{N}N$ interaction needed for studies of FSI effects on the timelike electromagnetic form factor of the proton is fairly well established. There is a wealth of empirical information on the elastic ($\bar{p}p \to \bar{p}p$) and charge-exchange ($\bar{p}p \to \bar{n}n$) reactions from direct scattering experiments and there is also a partial-wave analysis available [18]. Thus, for our own investigation we could build on a $\bar{N}N$ potential derived within chiral effective field theory, fitted to the results of the PWA [17]. The situation for the $\bar{\Lambda}\Lambda$ is very different, specifically in this case scattering experiments are impossible. Indeed, the only constraints we have for the $\bar{\Lambda}\Lambda$ force come from the FSI in the reaction $\bar{p}p \to \bar{\Lambda}\Lambda$. This reaction has been thoroughly studied in the PS185 experiment and data are available for total and differential cross-sections but also for polarization (P) and spin-correlation parameters (C_{ij}) [26,27,29], down to energies very close to the reaction threshold, see also the review in Ref. [28].

The reaction $\bar{p}p \to \bar{\Lambda}\Lambda$ has been analyzed in various model studies, where the strangeness production process is described either in terms of the constituent quark model [37–39] or by the exchange of strange mesons [30,32]. In the Jülich meson-exchange model the hyperon-production reaction is considered within a coupled-channel approach. This allows one to take into account rigorously the effects of the initial ($\bar{p}p$) and final ($\bar{\Lambda}\Lambda$) state interactions. The microscopic strangeness production process and the elastic parts of the interactions in the $\bar{p}p$ and $\bar{\Lambda}\Lambda$ systems are described by meson exchanges, while annihilation processes are accounted for by phenomenological optical potentials. To be specific, the elastic parts of the $\bar{p}p$ and $\bar{\Lambda}\Lambda$ interactions are G-parity transforms of an one-boson-exchange variant of the Bonn NN potential [40] and of the hyperon–nucleon model A of Ref. [41], respectively. The parameters of the $\bar{p}p$ annihilation potential are fixed by an independent fit to $\bar{p}p$ data in the energy region relevant for $\bar{\Lambda}\Lambda$ production while those for $\bar{\Lambda}\Lambda$ are determined by a fit to the $\bar{p}p \to \bar{\Lambda}\Lambda$ observables. As documented in Refs. [30,32], the model achieved a fairly good overall description of the PS185 data.

In the present study we use the $\bar{\Lambda}\Lambda$ potentials I, II, and III of Ref. [30] (cf. Table III) and K and QG from Ref. [32] (Table II). The models differ by variations in the employed parameterization of the $\bar{N}N$ annihilation potential and by differences in the $\bar{p}p \to \bar{\Lambda}\Lambda$ transition mechanism. Total cross sections for $\bar{p}p \to \bar{\Lambda}\Lambda$ of the considered potentials agree with each other and with the experiment up to $p_{\rm lab} \approx 1700$ MeV (corresponding to $\sqrt{s} \approx 2.32$ GeV or an excess energy $Q = \sqrt{s} - 2m_\Lambda$ of about 90 MeV). However, the spin-dependent observables are not always reproduced quantitatively. Still we believe that it is useful to employ all models in the present study because this allows us to shed light on the (unavoidable) model dependence of our predictions for the electromagnetic form factor of the Λ in the timelike region.

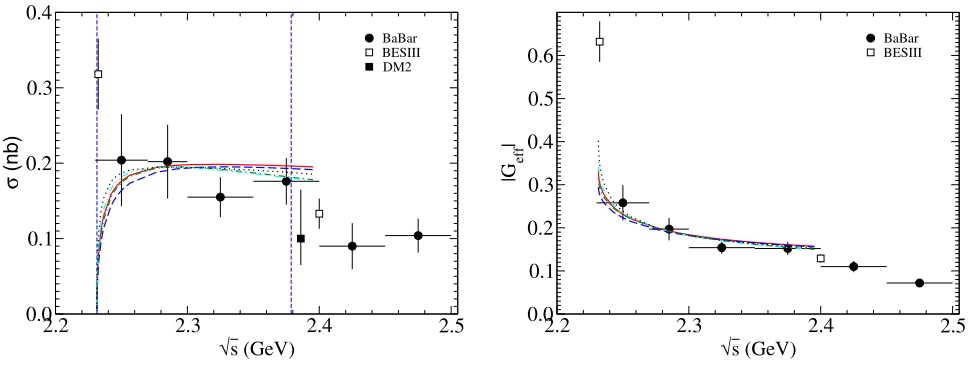

Fig. 1. Total cross section (left) and effective form factor $|G_{\rm eff}|$ (right) for $e^+e^- \to \bar{\Lambda}\Lambda$. Data are from the DM2 [19], BaBar [20], and BESIII [22] collaborations. Note that the latter data are still preliminary. The vertical lines indicate the $\bar{\Lambda}\Lambda$ and $\overline{\Sigma^+}\Sigma^+$ thresholds, respectively. The solid, dashed, and dash-dotted lines correspond to the $\bar{\Lambda}\Lambda$ models I, II, and II from Ref. [30], the dash-double-dotted and dotted lines to the models K and Q described in Ref. [32].

4. Results and discussion

Results for the $e^+e^- \to \bar{\Lambda}\Lambda$ cross section are depicted in Fig. 1 (left panel). The $\bar{\Lambda}\Lambda$ threshold is at $\sqrt{s} = 2.23138$ GeV in our calculation. We normalized the various curves to yield the same value at the maximum (i.e. roughly 0.2 nb) so that one can easily compare the differences in the energy dependence. The overall normalization, corresponding to the value of the bare electromagnetic form factors G_M^0 and G_E^0, is actually the only free parameter in our calculation, see Ref. [14]. Obviously, for all $\bar{\Lambda}\Lambda$ models the cross section rises rather sharply from the threshold and then remains practically constant for the next 100 MeV or so. This behavior is very well in line with the experimental information from the BaBar collaboration [20]. There are quantitative differences between the predictions of the different $\bar{\Lambda}\Lambda$ potentials considered but it is reassuring to see that, overall, the model dependence is fairly moderate.

Thus, it seems that despite of all the uncertainties in the dynamics reflected in the various considered $\bar{\Lambda}\Lambda$ models, the data on $\bar{p}p \to \bar{\Lambda}\Lambda$ put fairly tight constraints on the properties of the $\bar{\Lambda}\Lambda$ interaction. However, equally or possibly even more important is presumably the fact that the $\bar{\Lambda}\Lambda$ FSI employed here incorporates some very essential features. First, it is generated by solving a scattering equation and, therefore, properly unitarized, and secondly it includes effects from the presence of annihilation channels. We believe that most likely those features alone fix already the qualitative behavior of the $e^+e^- \to \bar{\Lambda}\Lambda$ near-threshold cross section. This conjecture is supported by the situation in the $e^+e^- \to \bar{p}p$ reaction. In this case the FSI is very different when it comes to details. For example, in the $\bar{N}N$ system there is a contribution from the important and long-ranged pion-exchange that creates a strong tensor force. In case of $\bar{\Lambda}\Lambda$ one pion exchange cannot contribute because of isospin symmetry. Still the near-threshold behavior of the $e^+e^- \to \bar{\Lambda}\Lambda$ and $e^+e^- \to \bar{p}p$ cross sections is rather similar, compare Fig. 1 here with Fig. 3 in Ref. [14] (cf. also Fig. 2 in [42] for $e^+e^- \to \bar{n}n$). It is remarkable that even the presence of the Coulomb interaction in the $\bar{p}p$ case, usually accounted for in terms of the Sommerfeld–Gamov factor [14], has very little impact on the qualitative similarity, despite the fact that it changes the threshold behavior of the $e^+e^- \to \bar{p}p$ reaction so that the cross section remains finite even at the nominal threshold.

Fig. 1 contains also two new and still preliminary data points from the BESIII collaboration [22] (open squares). Those data suggest a very different trend for the energy dependence of $\sigma_{e^+e^- \to \bar{\Lambda}\Lambda}$. Specifically, a large finite value for the cross section practically at the threshold is suggested. This cannot be reproduced by our calculation because the phase-space factor β (see Eq. (2)) enforces the cross section to go to zero linearly with the cms momentum k_Λ of the $\bar{\Lambda}\Lambda$ system. There is no Coulomb interaction here that would change the threshold behavior. The only possibility could be a very narrow resonance sitting more or less directly at the threshold which would then allow to overrule the k_Λ behavior from the phase space alone. Including such a threshold resonance in our $\bar{\Lambda}\Lambda$ potentials would, however, completely spoil the agreement with the $\bar{p}p \to \bar{\Lambda}\Lambda$ experiments. Anyway, one has to wait simply on the final results of the BESIII measurement. Interestingly, initial data for $\bar{p}p \to \bar{\Lambda}\Lambda$ suggested that there could be a near threshold resonance in the $^3S_1$ $\bar{\Lambda}\Lambda$ state [43]. However, a later high-statistics measurement by Barnes et al. [27] ruled that out convincingly. This experiment scrutinized the 5 MeV sector adjacent to the $\bar{\Lambda}\Lambda$ threshold with an unprecedented resolution of 0.2 MeV.

For illustration purposes we show results up to the $\overline{\Sigma^+}\Sigma^+$ threshold (indicated by a vertical line). However, we expect that near that threshold $e^+e^- \to \bar{\Sigma}\Sigma \to \bar{\Lambda}\Lambda$ two-step processes will become important, which are not included, and, therefore, our calculation is certainly no longer valid at those energies. In this context it is interesting to note that, indeed, the data suggest a certain drop in the $e^+e^- \to \bar{\Lambda}\Lambda$ cross section right above the $\overline{\Sigma^+}\Sigma^+$ threshold, cf. Fig. 1 (left). In reality we would estimate the validity range of the predictions to about 100 MeV from the threshold, i.e. up to $\sqrt{s} \approx 2.32$ GeV. This is the energy range where the $\bar{p}p \to \bar{\Lambda}\Lambda$ data are described by the potentials and it is also the range where we know from the $e^+e^- \to \bar{p}p$ case that FSI effects are relevant and determine the energy dependence of the observables [14]. Over a larger energy region, the intrinsic energy and momentum dependence of the $\bar{\Lambda}\Lambda$ production mechanism itself should become more significant or even dominant and then the present assumption that the bare electromagnetic form factors G_M^0 and G_E^0 that enter our calculation are constant is not valid anymore, see Eq. (10) of Ref. [14] for more details.

Predictions for the Λ effective form factor $G_{\rm eff}$ are presented in the right panel of Fig. 1. Since that quantity differs from the cross section only by kinematical factors, see Eq. (3), it is not surprising that our results are again in line with the corresponding empirical information deduced from the experiments cross sections [20]. Once again one can see that the preliminary near-threshold data point from BESIII differs drastically from the general trend.

Results for the form factor ratio $|G_E/G_M|$ and the relative phase between G_E and G_M are presented in Fig. 2. Clearly, those quantities are much more model-dependent and specifically for the phase there are fairly large variations between the predictions from the $\bar{\Lambda}\Lambda$ potentials considered. The experimental results for $|G_E/G_M|$ from Ref. [20] are also shown. The lower mass resolution of that quantity does not allow any more concrete conclusions. However, the trend that the ratio is somewhat larger than 1 for

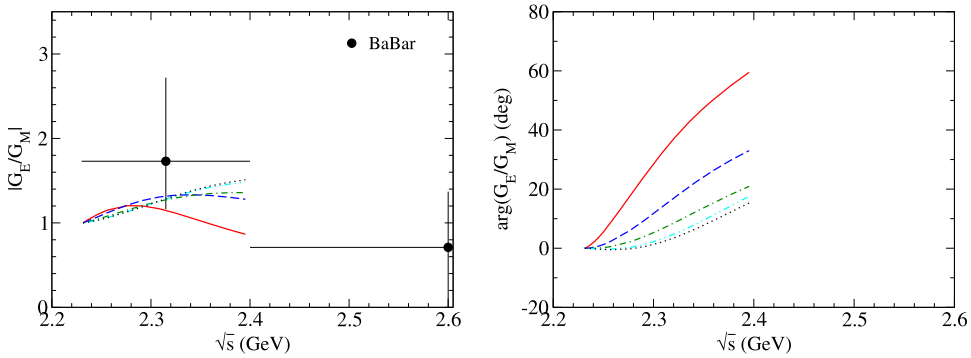

Fig. 2. The ratio $|G_E/G_M|$ (left) and phase $\phi = \arg(G_E/G_M)$ (right) as a function of the total cms energy. Data are from Ref. [20]. For notation, see Fig. 1.

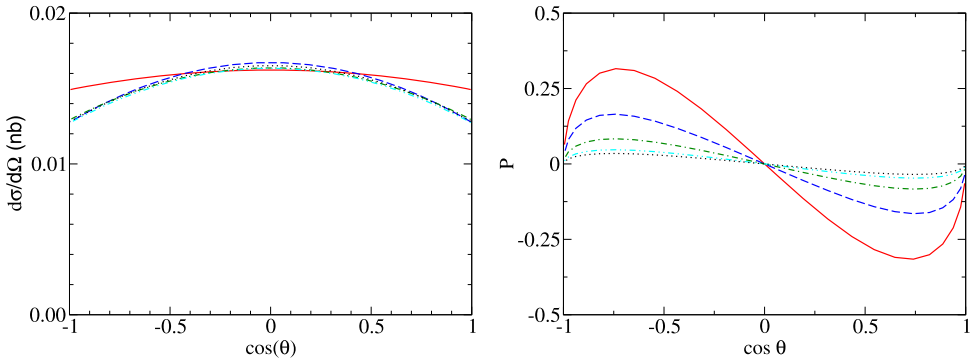

Fig. 3. Differential cross section (left) and polarization (right) for $e^+e^- \to \bar{\Lambda}\Lambda$ at the excess energy $Q = 90$ MeV ($\sqrt{s} = 2.32$ GeV). For notation, see Fig. 1.

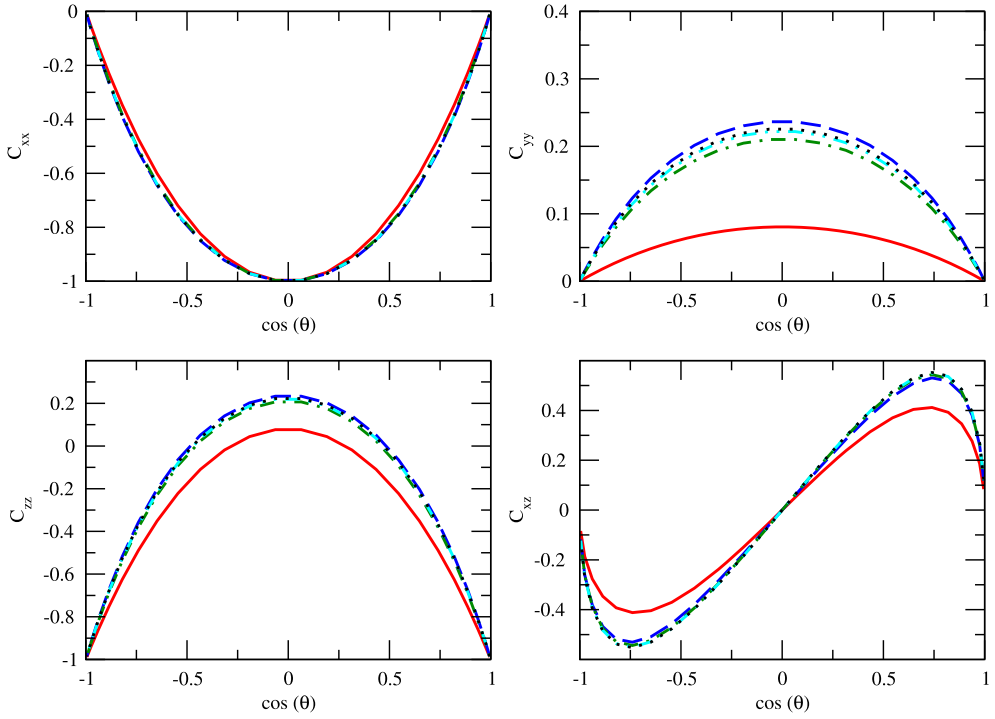

Fig. 4. Spin correlations parameters for $e^+e^- \to \bar{\Lambda}\Lambda$ at the excess energy $Q = 90$ MeV ($\sqrt{s} = 2.32$ GeV). For notation, see Fig. 1.

smaller energies and possibly smaller than 1 for larger energies is also suggested by most of the $\bar{\Lambda}\Lambda$ potentials. Let us also mention that the relative phase between G_E and G_M was determined to be in the range $-0.76 < \sin\phi < 0.98$ by the BaBar collaboration [20].

Finally, and in anticipation of pertinent results from the BESIII collaboration [22,25], in Figs. 3 and 4 we present exemplary predictions for the differential cross section and for polarization observables at an excess energy of 90 MeV. As discussed above, this energy might be alrighty close to the limit of validity of our calculation. However, at higher energies there is a stronger model dependence and we believe that it is instructive to see how the resulting differences, already discussed in the context of the form

factors G_E and G_M, manifest themselves directly in the actual observables accessible in the experiment. A view on the sensitivity of specific observables to variations of the $\bar{\Lambda}\Lambda$ interaction, or equivalently of G_M and G_E, could be quite helpful for planning future experiments.

Among the observables presented in Figs. 3 and 4 the polarization P exhibits the strongest variation with the employed $\bar{\Lambda}\Lambda$ interaction. This is not surprising because P is proportional to $\mathrm{Im}(G_M\, G_E^*)$, see [24], i.e. it depends strongly on the relative phase between G_M and G_E, and we have seen above that there are sizable differences in the prediction for this quantity. The spin-correlation parameter C_{xz} is proportional to $\mathrm{Re}(G_M\, G_E^*)$ [24] and, therefore, reflects mainly variations in the ratio $|G_E/G_M|$. These variations are also visible in C_{yy} which is sensitive to the difference $|G_M|^2 - |G_E|^2$.

Note that the sign of some polarization observables depends on the choice of the reference frame. As said in Sec. 2, we adopt here the formalism described in the Appendix of Ref. [32]. The spin-observables are calculated in the $\bar{\Lambda}\Lambda$ coordinate system, i.e. the direction of the $\bar{\Lambda}$ is defined as z direction. This agrees with the one employed in the PS185 experiment in the analysis of the $\bar{p}p \to \bar{\Lambda}\Lambda$ reaction [26]. The spin observables in Ref. [24] have partly opposite signs, in particular $A_y = -P$, $A_{xx} = -C_{xx}$, and $A_{zz} = -C_{zz}$.

As already noted above, we believe that the similar properties of the near-threshold cross sections for $e^+e^- \to \bar{\Lambda}\Lambda$ and $e^+e^- \to \bar{p}p$, consisting in a sharp rise and then a practically constant behavior, can be understood in terms of FSI effects driven by qualitative aspects that are common to the $\bar{\Lambda}\Lambda$ and $\bar{p}p$ interactions, like unitarity and the presence of annihilation processes. Available data for $\bar{p}p \to \bar{\Sigma}^0\Lambda$ and $\bar{p}p \to \bar{\Sigma}^0\Sigma^0$ from the BaBar collaboration [20] suggest likewise such a behavior. However, since the mass resolution of the data for those reactions is significantly lower one cannot draw firm conclusions at the moment. There are data with comparable resolution (i.e. 20 MeV/c^2) for the reaction $e^+e^- \to \bar{\Lambda}_c\Lambda_c$ from the Belle collaboration [44]. Those data were analyzed by us in Ref. [45] and it was found that the inclusion of FSI effects (based on a $\bar{\Lambda}_c\Lambda_c$ interaction derived from the $\bar{\Lambda}\Lambda$ interactions employed in the present study by invoking SU(4) flavor-symmetry arguments [46]) improves the description of the data in the threshold region. On the other hand, in this reaction the near-threshold invariant mass spectrum is dominated by the so-called $X(4630)$ resonance and, therefore, exhibits a behavior that clearly differs from the ones in the $\bar{p}p$ and $\bar{\Lambda}\Lambda$ channels.

5. Summary

In the present paper we investigated the reaction $e^+e^- \to \bar{\Lambda}\Lambda$ in the near-threshold region with specific emphasis on the role played by the interaction in the final $\bar{\Lambda}\Lambda$ state. The calculation is based on the one-photon approximation for the elementary reaction mechanism, but takes into account rigorously the effects of the $\bar{\Lambda}\Lambda$ interaction in close analogy to our work on $e^+e^- \to \bar{p}p$ [14]. For the $\bar{\Lambda}\Lambda$ interaction we utilized a variety of potentials that were constructed for the analysis of the reaction $\bar{p}p \to \bar{\Lambda}\Lambda$ about two decades ago [30,32]. Those potentials are basically of phenomenological nature but fitted and constrained by the wealth of near-threshold data on $\bar{p}p \to \bar{\Lambda}\Lambda$ taken in the PS185 experiment at LEAR [28].

The energy dependence of the near-threshold $e^+e^- \to \bar{\Lambda}\Lambda$ cross section reported by the BaBar collaboration [20], which consists in a sharp rise from the threshold and then a flat behavior for the next 100 MeV or so, is well reproduced by our calculation based on the various $\bar{\Lambda}\Lambda$ potentials. Most likely, general features like that the employed FSI is generated by solving a scattering equation (and, therefore, properly unitarized) and that it includes effects from the presence of annihilation channels fix the qualitative behavior of the $e^+e^- \to \bar{\Lambda}\Lambda$ near-threshold cross section so that there is only a moderate model dependence. Indeed the situation is very similar to the one in the $e^+e^- \to \bar{p}p$ reaction where the measured near-threshold cross section shows a comparable behavior and where likewise FSI effects are able to account for this [14].

Preliminary results from the BESIII collaboration indicate a very much different energy dependence of the $e^+e^- \to \bar{\Lambda}\Lambda$ cross section [22]. If that behavior is confirmed in the final analysis it will be very difficult to reconcile the e^+e^- results with our knowledge on the $\bar{p}p \to \bar{\Lambda}\Lambda$ reaction [28]. Note that the latter is also completely dominated by the $^3S_1$ partial wave close to threshold [26, 30] and thus by exactly the same $\bar{\Lambda}\Lambda$ FSI. In any case, further data in the near-threshold region with better mass resolution would be very helpful to resolve this issue.

Finally, due to the self-analyzing character of the weak Λ decay the polarization as well as spin-correlation parameters for the reaction $e^+e^- \to \bar{\Lambda}\Lambda$ can be determined, in close analogy to what has been already achieved in the PS185 experiment for $\bar{p}p \to \bar{\Lambda}\Lambda$ [28]. We are looking forward to analyze such data within our formalism, once they become available, because they will certainly allow one to put much tighter constraints on the interaction in the $\bar{\Lambda}\Lambda$ system.

Acknowledgements

We acknowledge stimulating discussions with Tord Johansson. This work is supported in part by the DFG (TRR 110) and the NSFC (11621131001) through funds provided to the Sino-German CRC 110 “Symmetries and the Emergence of Structure in QCD”. The work of UGM was also supported by the Chinese Academy of Sciences (CAS) President’s International Fellowship Initiative (PIFI) (Grant No. 2015VMA076).

References

[1] A. Denig, G. Salmè, Prog. Part. Nucl. Phys. 68 (2013) 113.
[2] G. Bardin, et al., Nucl. Phys. B 411 (1994) 3.
[3] B. Aubert, et al., Phys. Rev. D 73 (2006) 012005.
[4] J.P. Lees, et al., Phys. Rev. D 87 (2013) 092005.
[5] M.N. Achasov, et al., Phys. Rev. D 90 (2014) 112007.
[6] M. Ablikim, et al., BESIII Collaboration, Phys. Rev. D 91 (2015) 112004.
[7] R.R. Akhmetshin, et al., CMD-3 Collaboration, Phys. Lett. B 759 (2016) 634.
[8] B. Singh, et al., PANDA Collaboration, arXiv:1606.01118 [hep-ex].
[9] J. Haidenbauer, H.-W. Hammer, U.-G. Meißner, A. Sibirtsev, Phys. Lett. B 643 (2006) 29.
[10] V.F. Dmitriev, A.I. Milstein, Phys. Lett. B 658 (2007) 13.
[11] R. Baldini, S. Pacetti, A. Zallo, A. Zichichi, Eur. Phys. J. A 39 (2009) 315.
[12] G.Y. Chen, H.R. Dong, J.P. Ma, Phys. Lett. B 692 (2010) 136.
[13] O.D. Dalkarov, P.A. Khakhulin, A.Y. Voronin, Nucl. Phys. A 833 (2010) 104.
[14] J. Haidenbauer, X.-W. Kang, U.-G. Meißner, Nucl. Phys. A 929 (2014) 102.
[15] I.T. Lorenz, H.W. Hammer, U.-G. Meißner, Phys. Rev. D 92 (2015) 034018.
[16] V.F. Dmitriev, A.I. Milstein, S.G. Salnikov, Phys. Rev. D 93 (2016) 034033.
[17] X.W. Kang, J. Haidenbauer, U.-G. Meißner, J. High Energy Phys. 1402 (2014) 113.
[18] D. Zhou, R.G.E. Timmermans, Phys. Rev. C 86 (2012) 044003.
[19] D. Bisello, et al., DM2 Collaboration, Z. Phys. C 48 (1990) 23.
[20] B. Aubert, et al., BaBar Collaboration, Phys. Rev. D 76 (2007) 092006.
[21] S. Dobbs, A. Tomaradze, T. Xiao, K.K. Seth, G. Bonvicini, Phys. Lett. B 739 (2014) 90.
[22] C. Morales Morales, BESIII Collaboration, AIP Conf. Proc. 1735 (2016) 050006.
[23] G. Fäldt, Eur. Phys. J. A 51 (2015) 74.
[24] G. Fäldt, Eur. Phys. J. A 52 (2016) 141.
[25] T. Johansson, private communication.
[26] P.D. Barnes, et al., Nucl. Phys. A 526 (1991) 575.
[27] P.D. Barnes, et al., Phys. Rev. C 62 (2000) 055203.
[28] E. Klempt, F. Bradamante, A. Martin, J.-M. Richard, Phys. Rep. 368 (2002) 119.
[29] K.D. Paschke, et al., Phys. Rev. C 74 (2006) 015206.
[30] J. Haidenbauer, T. Hippchen, K. Holinde, B. Holzenkamp, V. Mull, J. Speth, Phys. Rev. C 45 (1992) 931.
[31] J. Haidenbauer, K. Holinde, V. Mull, J. Speth, Phys. Lett. B 291 (1992) 223.

[32] J. Haidenbauer, K. Holinde, V. Mull, J. Speth, Phys. Rev. C 46 (1992) 2158.
[33] J. Haidenbauer, K. Holinde, J. Speth, Nucl. Phys. A 562 (1993) 317.
[34] J. Bystricky, F. Lehar, P. Winternitz, J. Phys. 39 (1978) 1.
[35] E. Tomasi-Gustafsson, F. Lacroix, C. Duterte, G.I. Gakh, Eur. Phys. J. A 24 (2005) 419.
[36] N.H. Buttimore, E. Jennings, Eur. Phys. J. A 31 (2007) 9.
[37] M. Kohno, W. Weise, Phys. Lett. B 179 (1986) 15.
[38] M.A. Alberg, E.M. Henley, L. Wilets, P.D. Kunz, Nucl. Phys. A 560 (1993) 365.
[39] P.G. Ortega, D.R. Entem, F. Fernandez, Phys. Lett. B 696 (2011) 352.
[40] J. Haidenbauer, K. Holinde, M.B. Johnson, Phys. Rev. C 45 (1992) 2055.
[41] B. Holzenkamp, K. Holinde, J. Speth, Nucl. Phys. A 500 (1989) 485.
[42] J. Haidenbauer, C. Hanhart, X.W. Kang, U.-G. Meißner, Phys. Rev. D 92 (2015) 054032.
[43] J. Carbonell, K.V. Protasov, O.D. Dalkarov, Phys. Lett. B 306 (1993) 407.
[44] G. Pakhlova, et al., Belle Collaboration, Phys. Rev. Lett. 101 (2008) 172001.
[45] F.K. Guo, J. Haidenbauer, C. Hanhart, U.-G. Meißner, Phys. Rev. D 82 (2010) 094008.
[46] J. Haidenbauer, G. Krein, Phys. Lett. B 687 (2010) 314.